

Paper

Enhancing Millimeter Wave Reflect Arrays with Thick LC Devices Utilizing Two-Direction Electric Field Driving

Ryo Aoyanagi†, Masakazu Nakatani†, Takahiro Ishinabe† (member),
Hiroyasu Sato†, Qiang Chen† and Hideo Fujikake† (fellow)

Abstract This study proposed a two-direction electric field driving method for thick-film liquid crystal devices aimed at the millimeter-wave phase modulation of reflected arrays. The findings illustrate that a meticulous electrode shape design and strategic exploitation of the elastic orientation behavior yield both heightened liquid crystal molecule responsiveness and augmented phase modulation capabilities.

Keywords: two-direction electric field-driving, reflect array, nematic liquid crystal, thick liquid crystal.

1. Introduction

Recent advancements beyond the 5G technology, which have resulted in faster data transmission and the ability to connect numerous devices simultaneously, have garnered significant attention. However, the limited coverage area of radio waves is a challenge faced by the evolution beyond 5G. This limitation arises from the weak diffraction of millimeter waves emitted from base stations, which hinders their reach into areas obstructed by structures, such as buildings. Reflective arrays (RA) have emerged as promising solutions for addressing this issue [1]. Fig. 1 illustrates the expanded coverage area achieved through the RA, and Fig. 2 presents a conceptual depiction of the RA setup. The RA comprises reflector elements arranged in a periodic array, with adjustments in the electrical length of each element, enabling control over the phase of the scattered waves, thereby facilitating arbitrary beam direction adjustments [2].

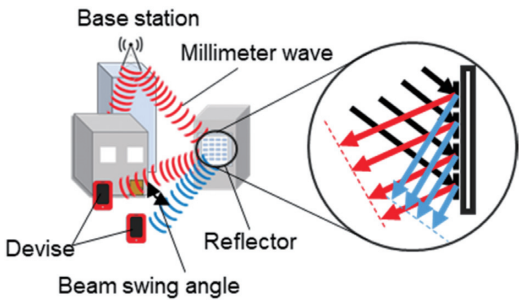

Fig. 1 Expansion of coverage area.

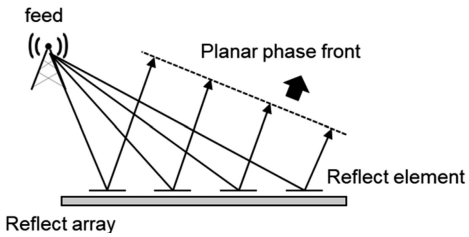

Fig. 2 Radio wave reflection.

An example of phase control involves a device that uses the diode switching-induced changes in the electrical length [3]. However, concerns have arisen regarding current distortion owing to diode rectification characteristics, potentially leading to harmonic generation and interference in other frequency bands. Consequently, our focus has shifted toward phase control using the dielectric anisotropy of nematic liquid crystals (LCs). This unique method involves beam control through alignment manipulation of LC molecules using a low-frequency alternating current (AC) voltage [4].

Nevertheless, achieving substantial changes in dielectric constant necessitates thick LC layers (50 μm or more), resulting in prolonged fall-response times of LC molecules, e.g., 170-190 s [5] and 290 s [6]. The switch-off time t_{off} of the nematic LC liquid crystals is strongly affected by the thickness d, as shown in the following equation: [7] [8]

$$t_{off} = \frac{\eta d^2}{k\pi^2} \quad (1)$$

Received March 31, 2024; Revised June 9, 2024; Accepted June 18, 2024
† Department of Electronics, Graduate School of Engineering, Tohoku University
(Sendai, Japan)

where η is the rotational viscosity of the LC, k is the appropriate expression for the elastic constant of the LC mixture.

To address this issue, methods employing polymer-stabilized LC (PSLC) [9] and polymer-dispersed LC (PDLC) [10] have been investigated. Cross-comb electrode methods have been proposed for this purpose. Examples include the interdigital gap method [11], and the terahertz in-plane and terahertz out-of-plane (TIP-TOP) method[12]. TIP-TOP method is two-directional electric field driving and adopt for phase shifter. A horizontal response time of 5.8 s was achieved using the TIP-TOP method. However, TIP-TOP method is not adopt for reflective array but adopt for phase shifter. If TIP-TOP method use for RA, very slow for 5G data transfer and further research is required on the electrode gap and LC direction.

Considering these challenges, we proposed a two-direction electric field driving device with a comb-type electrode substrate on one side of the LC layer and study the directional characteristics of the electrode gap and LC.

This design aims to facilitate swift response times, mitigate the driving voltage demands, and ensure adequate phase modulation. This study introduces an LC device featuring this two-direction electric field driving structure, and the evaluation focuses on the fundamental behavior of LC orientation changes within the fabricated device.

2. Operating principle of two-direction electric field drive structure

Fig. 3 illustrates the movement of a thin and thick LC. Specifically, Fig. 3(a) shows a thin LC immediately after the applied voltage is OFF. Fig. 3(b) shows a thin LC the thin LC in stable state. Fig. 3(c) shows a thicker LC with an applied ON voltage, whereas Fig. 3(d) shows a thicker LC immediately after the applied voltage is OFF. Furthermore, Fig. 3(e) shows the thick-film LC in a stable state after certain time has elapsed because the voltage is turned off. The reorientation mechanism in conventional LC devices relies on the alignment of surface-generated regulatory forces of the film. As shown in Fig. 3(a), many LCs in thin structures are affected by the alignment film. Therefore, the LC becomes stable early, and the response speed is fast. In the other hand, as shown in Fig. 3(d), the center of the thick LC experienced a weak force from the alignment layer, which reduced the fall response time. The fall response time was correlated with the square of the LC layer thickness.

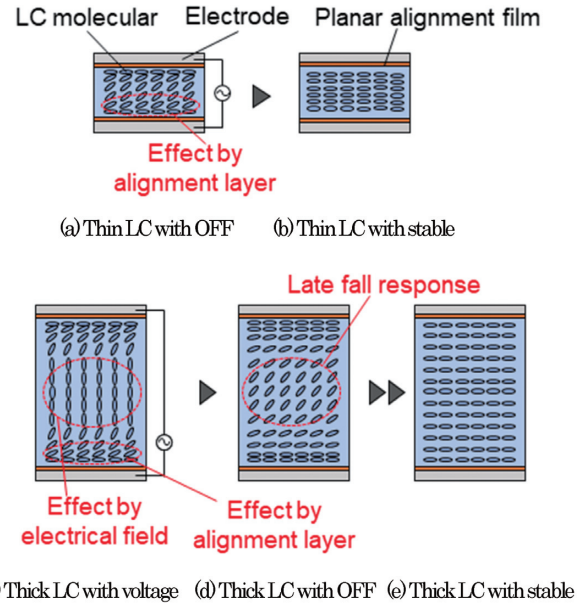

Fig. 3 Movement in thicker LC.

This section elucidates the operating principle of the two-direction electric field driving device, as depicted in Fig. 4.

As illustrated in Fig. 4(a) and (b), a low-frequency AC power supply was connected. As shown in Fig. 4(a), an electric field was applied vertically during the elevation of LC molecules. Conversely, a horizontal electric field was applied between the upper right and left electrodes during the descent from the vertical orientation state to the initial orientation, as illustrated in Fig. 4(b). These applied electric fields expedite the fall response, which is a characteristic of the proposed two-direction electric-field driving device. Moreover, as no polymer materials

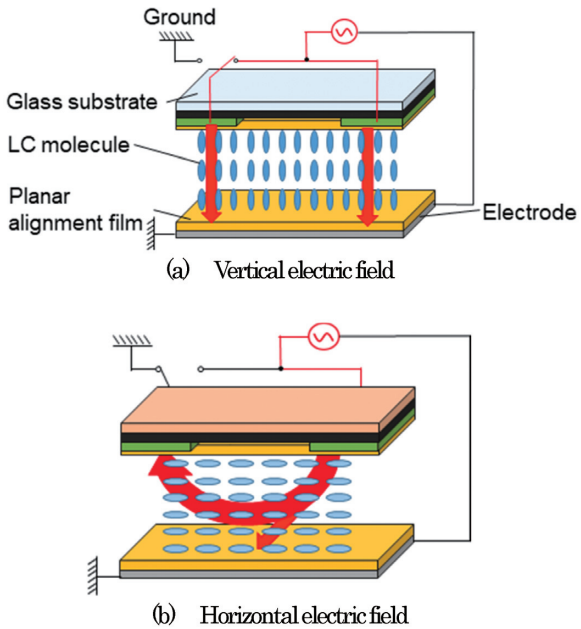

Fig. 4 Schematic of two-direction electric field driving structure.

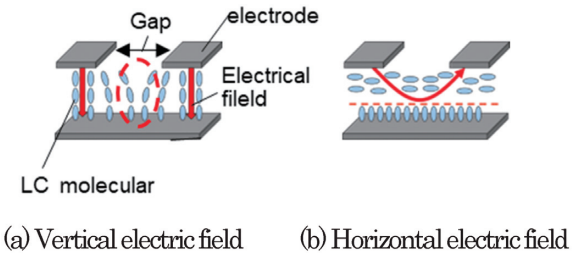

Fig. 5 Movement of LC and electric field in two-direction electric field driving.

were introduced in the LC layer, a reduction in driving voltage was anticipated, as discussed in the preceding section. However, as shown in Fig. 5(a), a low electric field was predicted between the upper right and left electrodes when voltage was applied to the vertical drive. Similarly, as shown in Fig. 5(b), a low electric field was predicted near the bottom electrode when a voltage was applied to the horizontal drive. The movement of an LC in such low electric field regions remains unexplored. Therefore, we examined the movement of an LC under electrode gap conditions.

3. Response time measurement using a two-direction electric field driving device

3.1 Structure of the elements

A glass substrate with comb-shaped electrodes was employed to fabricate a two-direction electric field-driving device, as shown in Fig. 6. The glass is soda-lime glass. Soda-lime glass has a higher loss of electromagnetic waves due to transmission than quartz, however soda-lime glass has sufficient transmission to validate RA. The electrode material was indium tin oxide, which is sufficiently thin to be considered transparent to millimeter waves. Here, the width of the comb-shaped electrode is referred to as the electrode width and the space between the electrodes is called the inter-electrode gap.

Planar alignment layers (AL1254) were applied to the comb and full-face electrode substrates, and nematic LC (E-7, LCC) was injected into empty cells fabricated with 50 μm thick Mylar film spacers. The planar alignment layers and positive nematic LC were used because planar alignment layers generally have stronger anchor strengths than vertical alignment layers. The dimensions of the comb electrodes were: inter-electrode gap: 10, 50 μm and electrode width: 10 μm. The 10, 50 μm electrode gaps were chosen to elucidate the difference between the electrode gaps in later simulation, and ITO patterns can easily be made with electrode gap of 10 μm or greater. To compare the response times, a planar alignment layer was applied to the solid electrode substrate, and an LC cell with solid top and bottom electrodes, which served as the reference sample, and was fabricated using the same process (this served as the reference sample).

3.2 System for measuring response times and experimental parameters

Fig. 7 shows a diagram of the measurement system. For the measurement of transmitted light intensity, an LC cell was placed between two polarizers with orthogonal polarization axes at 45° to the polarization axis, and light from a halogen lamp was irradiated onto the device. The light transmitted through the LC layer is converted into a voltage waveform and observed. Furthermore, the change in the transmitted light intensity when the direction of the electric field was applied to the LC layer was measured using a sensitive charge-coupled device (CCD) camera. The response time was determined from the change in the transmitted light intensity when the electric field driving element was switched in both directions. Moreover, a square-wave voltage of 30 Vrms, 1 kHz, and a duty ratio of 50% were applied.

The response time when the direction of the electric field applied to the LC layer switches from horizontal to vertical is defined as the vertical-field response time. In

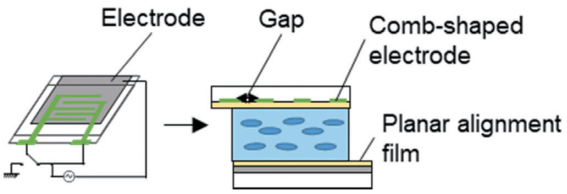

Fig. 6 Model of two-direction electric field driving device.

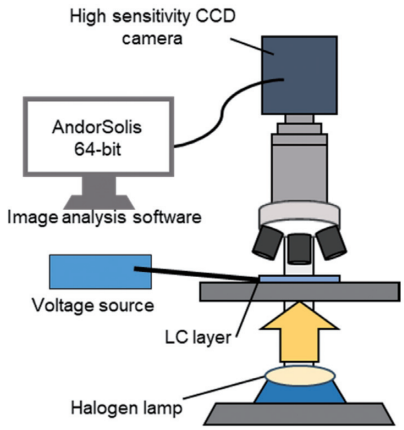

Fig. 7 Measurement system diagram.

contrast, the horizontal field response time was defined as the time when the direction was switched from vertical to horizontal. The driving voltage was set, and the response time was evaluated when the change in light intensity converged to 90% or more after voltage application.

3.3 Assessment of response time measurement outcomes

The response times of the reference samples are listed in Table 1. Additionally, Fig. 8 shows the time characteristics of the transmitted light intensity when vertical and horizontal electric fields were applied. The light intensities in Fig. 8 were normalized to the horizontal driving-light intensities. The response times ranged between 10% and 90%, where 0% and 100% correspond to the minimum and maximum light intensities, respectively.

Table 1 Summary of response time.

Reference sample		Rise response	105 (ms)
		Fall response	24 (s)
Two-direction electric field driving device	Gap 10 μm	Vertical	177.3 (ms)
		Horizontal	3.0 (ms)
	Gap 50 μm	Vertical	35 (ms)
		Horizontal	49 (ms)

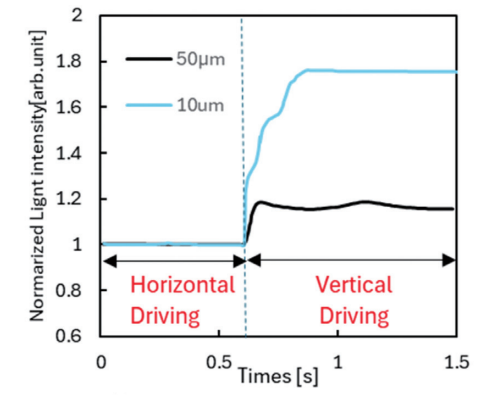

(a) Vertical electric field response

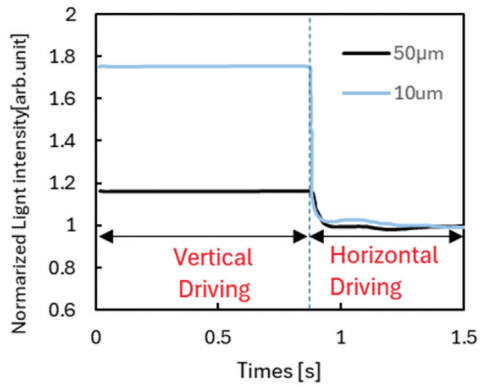

(b) Horizontal electric field response

Fig. 8 Light intensity vs. time characteristics.

The duration of response to vertical fields in the two-direction electric field driving device were 177 ms for 10 μm gap, as depicted by the blue lines, and 35 ms for 50 μm gap, as depicted by the black lines in Fig. 8(a) and (b). In contrast, horizontal field responses were 3 ms for 10 μm gap, as depicted by the blue line, and 49 ms for 50 μm gap, as depicted by the black line in Fig. 8(b). The horizontal field responses in 50 μm gap is 480 times faster than the fall response in reference sample, and 100 times firster than former TIP-TOP method phase shifter [12]. These findings confirm that applying a voltage during the falling edge accelerates the reorientation of the LC molecules.

However, based on the aforementioned outcomes, the responses to horizontal electric fields in the device with a 50 μm inter-electrode gap were approximately 16 times longer than those in the device with a 10 μm gap. This prolonged duration may stem from the heightened ratio of LC molecules influenced by the electric field, accompanied by an increase in the number of molecules undergoing elastic alignment.

4. Evaluation of LC orientation state

We evaluated the alignment condition within a two-direction electric field driving device using the LCDMaster2D (Shintech) software that employs numerical simulations based on the elastic body theory of LCs. The simulation conditions are listed in Table 2. Figs. 9 and 10 illustrate the hue distributions of the LC

Table 2 Simulation condition.

Pretilt angle (deg)	1
Anchoring strength (J/m^2)	10×10^6
Elastic constants (pN)	K_{11} 11 K_{22} 10.2 K_{33} 16.2
Dielectric constants (low frequency)	$\varepsilon_{\parallel}$ 19.6 $\varepsilon_{\perp}$ 5.1

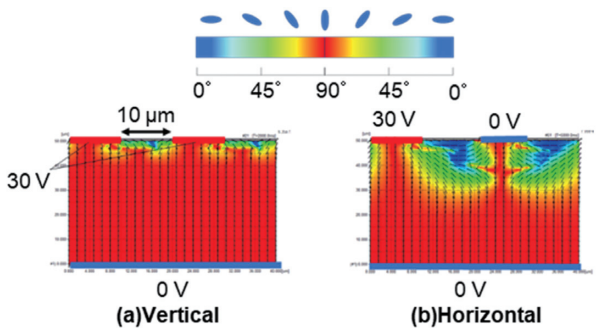

Fig. 9 Hue distribution image in the director direction (Gap10 μm).

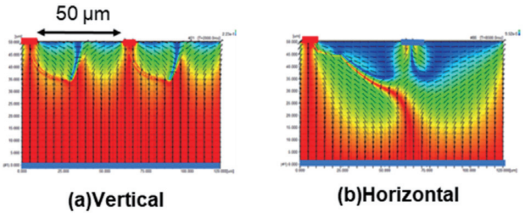

Fig. 10 Hue distribution image in the direction of the director (Gap50 μm).

molecules corresponding to their director tilt angles. The LC is asymmetric because its boundaries have a pretilt angle. The average tilt angles of the LC molecules, calculated through image analysis of the hue distributions shown in Figs. 9 and 10, are summarized in Table 3. Since the thickness of the LC layer is small compared to the wavelength, the LC layer can be considered as a capacitor, and the incident high-frequency electric and magnetic fields are assumed to be directed in the thickness direction. Therefore, we evaluated the LC molecular angles in the direction of the thickness.

Table 3 lists that the discrepancy in the average tilt angle of the LC molecular director between vertical and horizontal electric fields at a 10 μm electrode gap was 4.9°. Conversely, at 30, 40, 50 μm gaps, those differences increased to 7.4°, 7.1°, 7.2°, indicating more pronounced movement of LC molecules at the larger gap. In traditional thin LC layers, sufficient phase modulation can be achieved through electric-field driving. However, in thicker LC layers, electric field penetration is limited, leading to internal LC movement via elastic alignment propagation.

A discussion of the results is presented in Fig. 11. When the gap between the electrodes was increased with a horizontal electric field, as depicted in Fig. 11 (b), the horizontal electric field spread in the thickness direction compared with the narrow gap shown in Fig. 11(a). The spread of the horizontal electric field drives the LC over a large area. However, when the bandgap between the electrodes was increased with a vertical electric field, as illustrated in Fig. 11(d), a low-electric-field region was formed between the upper electrodes, as shown in Fig. 11(c). In this case, the effect of elasticity became dominant, resulting in a lower response speed.

Table 3 Dielector mean tilt angle of LC molecules.

	Vertical average Inclination angle(deg)	Horizontal average Inclination angle (deg)	Average Inclination angle difference (deg)
Gap 10 μm	88.1	83.2	4.9
Gap 20 μm	86.9	80.9	5.9
Gap 30 μm	85.8	78.4	7.4
Gap 40 μm	84.8	77.8	7.1
Gap 50 μm	83.7	76.5	7.2

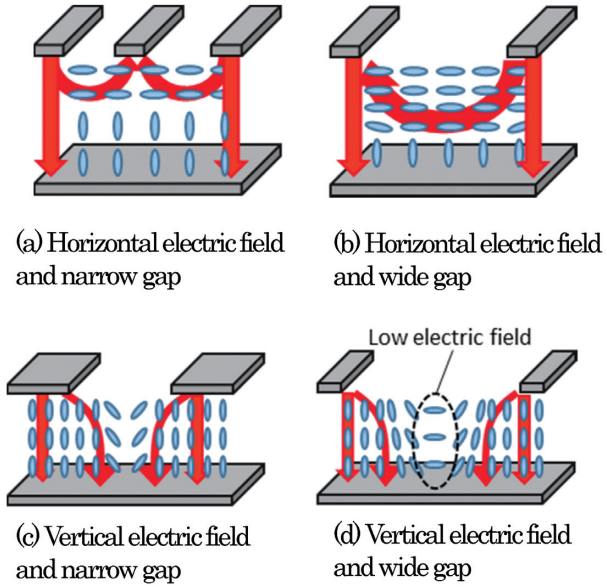

Fig. 11 Movement differences between narrow-gap and wide-gap LC.

These results confirm the existence of a tradeoff between the change in the dielectric constant and the response time at the gap length between the electrodes.

5. Millimeter Wave Characteristic Analysis

In this section, we analyze and evaluate the electric field distribution and zeroth-order reflected wave characteristics when millimeter waves are irradiated onto an RA with a two-direction electric field driving device using an LC orientation and a reflected electromagnetic wave analysis simulator (LC-RP Analyzer, Shintech Corp.). The analysis was conducted based on the exact coupled wave theory. Simulations were performed for a device featuring a two-direction drive structure implemented in an actual RA. The structural design is shown in Fig. 12. This simulation uses infinity periodic structure to x direction for millimeter wave. The liquid crystal simulation performed only at center unit by calculation limit. The incidence of the electric field was directly above of the RA. Polarization was linear and perpendicular to the comb electrode. The pretilt angle, anchoring strength,

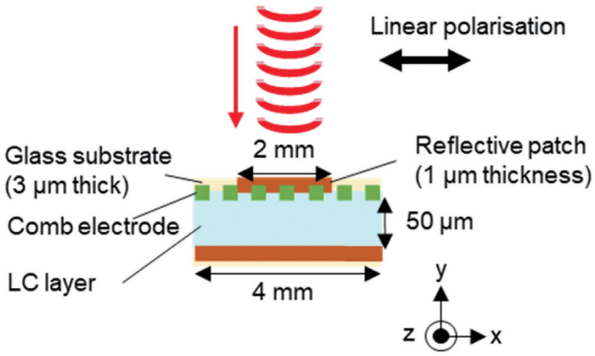

Fig. 12 Structural design of RA elements in simulation.

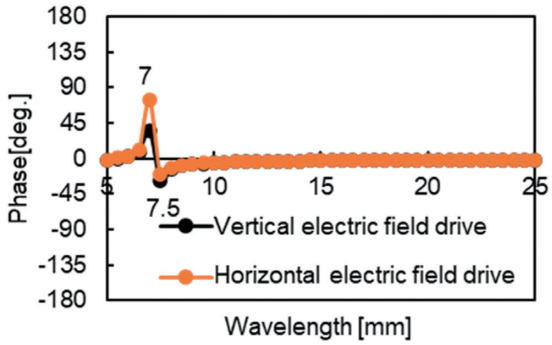

Fig.14 Wavelength-phase property.

Table 4 LC RA simulation conditions.

	Dielectric constant [-]	Dielectric loss tangent (tan δ)
LC(E-7) 19 GHz (wavelength 15.8 mm)[13]	$\varepsilon_{\parallel}$: 2.98 $\varepsilon_{\perp}$: 2.53	$tan\delta_{\parallel}$: 0.09 $tan\delta_{\perp}$: 0.022
Glass substrate	3.9	1.0×10^{-4}

and elastic constants are the same as in Table. 2. The dielectric constant and dielectric loss tangent at 19 GHz (wavelength of 15.8 mm) are listed in Table 4. [13]. Copper was used as the combing electrode which conductivity is 5.8×10^{7} [S/m]. .

Initially, the intensity distribution of the high-frequency electric field near the LC layer was examined for the reflected waves. An image of the hue distribution corresponding to the electric field intensity is shown in Fig. 13. This illustrates that the electric field is strong at both ends of the reflected patch and its lower part at a wavelength of 7 mm. This observation suggests that the electromagnetic waves were absorbed inside the LC layer, confirming a resonance phenomenon unique to the antenna.

The wavelength-phase modulation characteristics of the calculated reflected zeroth-order diffraction wave in the far field were investigated when the element was irradiated with millimeter waves. Fig. 14 shows a graph of each electric field direction in the proposed method. The graph demonstrates that the phase modulation occurred at a resonance wavelength of approximately 7 mm. The phase modulation at a wavelength of 7 mm was 34.9 (deg.) when a vertical field was applied. The phase modulation at the wavelength of 7 mm was 73.5 (deg.) when a horizontal electric field was applied. These results indicate that a larger phase modulation is obtained when a horizontal electric field is applied.

Fig.15 shows the reflectance of the proposed device when the irradiation wavelength was varied. The reflectance was decreased by driving the horizontal electric field. The relationship between reflectance and impedance is given as follows [14]:

$$\Gamma = \frac{(Z_2 - Z_1)^2}{(Z_2 + Z_1)^2} \tag{2}$$

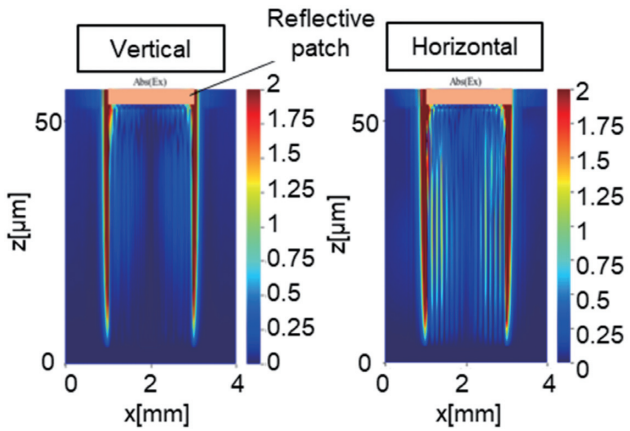

Fig.13 Distribution of high-frequency electric field in the LC layer.

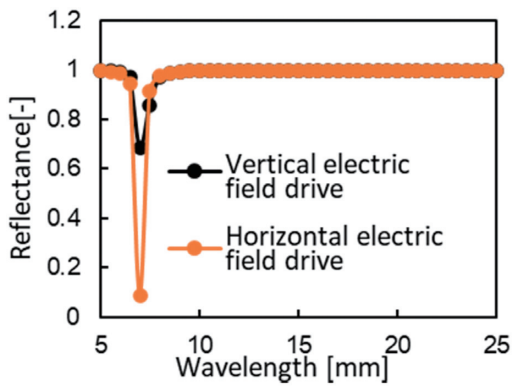

Fig.15 Wavelength-Reflectance characteristics.

where, Z_1 is the air impedance; Z_2 is the impedance of the liquid crystal The dielectric constant increases with horizontal and electric field incidence . This equation shows that as the impedance difference between the liquid crystal impedance and air increases, the reflectance decreases. The reflectance decreases at a wavelength of 7 mm, which matches the decrease in the reflectance and resonance wavelengths of this formula.

These results indicate that the phase of an incident millimeter-wave of a specific wavelength can be modulated by driving the LC using a unidirectional electric field driving device.

6. Conclusions

This study introduces a method for fabricating thick-film LC devices for millimeter-wave phase modulation using an electrode structure in which LC molecules are driven by a bidirectional electric field. The proposed structure is expected to accelerate the fall response of thick-film LCs. In addition, the LC orientation and reflected wave behavior of the fabricated devices were evaluated using simulations. Our findings demonstrate that the proposed method offers guidance for enhancing the dielectric constant change and enables the phase modulation of reflected millimeter waves.

7. Acknowledgements

The authors express their gratitude to Dai Nippon Printing Co., Ltd. for providing the mold. Additionally, the authors extend their gratitude to Assistant Professor Yosei Shibata of Nagaoka University of Technology for their valuable discussions. This study was supported by the Ministry of Internal Affairs and Communications of Japan (grant number JPJ000254).

References

1) D.M. Pozar, S.D. Targonski and H.D. Syrigos,:"Design of Millimeter Wave Microstrip Reflectarrays," IEEE Trans Antennas Propag, 45, 2, pp.287-296 (1997)
2) S. Zhang and R. Zhang: "Capacity Characterization for Intelligent Reflecting Surface Aided MIMO Communication," IEEE Journal on Selected Areas in Communications, 38, . 8, pp.1823-1838 (2020)
3) Sean V.Hum: "Realizing an Electronically Tuable Reflectarray Using Varactor Diode-Tuned Elements", IEEE Microwave and Wireless components letters, 15, 6, pp.422-424(2005)
4) M.Y. Ismail and R. Cahill: "Beam steering reflectarrays using liquid crystal substrate," in IEEE High Frequency Postgraduate Student Colloquium, vol. 2005, pp.62-65 (2005)
5) Cho-Fan Hsieh, Ru-Pin Pan, Tsung-Ta Tang, Hung-Lung Chen and Ci-Ling Pan "Voltage controlled liquid-crystal terahertz phase shifter and quarter-wave plate,", OPTICS LETTERS, 8, pp.1112-1114 (2006)
6) Chia-Jen Lin, Chuan-Hsien Lin, Yu-Tai Li, Ru-Pin Pan and Ci-Ling Pan, "Electrically controlled liquid crystal phase grating for terahertz waves." IEEE Photonics Technology Letters 21.11 p.p. 730-732 (2009)
7) Schadt, Martin. "Liquid crystal materials and liquid crystal displays." Annual review of materials science 27.1 p.p. 305-379 (1997)
8) E Jakeman, EP Raynes. "Electro-optic response times in liquid crystals." Physics Letters A 39.1 p.p. 69-70 (1972)
9) H. Fujikake, T. Kuki, T. Nomoto, Y. Tsuchiya and Y. Utsumi: "Thick polymer-stabilized liquid crystal films for microwave phase control," Appl Phys, 89, 10, pp.5295-5298 (2001)
10) Y. Utsumi, T. Kamei, K. Saito and H. Moritake: "Increasing the speed of microstrip line-type PDLC devices," IEEE MTT-S International Microwave Symposium Digest, 2005, pp.1831-1834 (2005)
11) J.F. Li, Q. Chen, Q.W. Yuan and K. Sawaya "Reflectarray element using interdigital gap loading structure." Electronics Letters 47.2, pp.83-85 (2011)
12) Benjamin S.-Y. Ung, Xudong Liu, Edward P.J. Parrott , Abhishek Kumar Srivastava, Hongkyu Park, Vladimir G. Chigrinov and Emma Pickwell-MacPherson "Towards a rapid terahertz liquid crystal phase shifter: Terahertz in-plane and terahertz out-plane (TIP-TOP) switching." IEEE Transactions on Terahertz Science and Technology 8.2, pp.209-214 (2018)
13) Fritzsch, Carsten, et al. "77Å]1: Invited Paper: Liquid Crystals beyond Displays: Smart Antennas and Digital Optics." SID Symposium Digest of Technical Papers. 50.,1, pp.1098-1101,,(2019)
14) Costa, Filippo and Agostino Monorchio. "Closed-form analysis of reflection losses in microstrip reflectarray antennas." IEEE transactions on antennas and propagation 60, 10, pp.4650-4660 (2012)

Ryo Aoyanagi received a B.E. degree from Tohoku University, Sendai, Japan, in 2022. He is a Master's student in the Department of Electronic Engineering at the Graduate School of Engineering, Tohoku University. His research interest is the two-direction electric field driving of thick Nematic LC Layer using LC-Polymer Films for Millimeter Wave Reflect Arrays.

Masakazu Nakatani received his M.S. in Engineering from Nara Institute of Science and Technology (NAIST) in March 2010 and Ph.D. in Engineering from Nagaoka University of Technology in December 2020. From 2010-2016, he joined Clean Venture 21, a low-concentration photovoltaics venture company, as a researcher; from 2020-2022, he worked as a postdoctoral researcher at Osaka University, studying light control by cholesteric liquid crystals. In February 2023, he joined Graduate School of Engineering, Tohoku University as an Assistant Professor.

Takahiro Ishinabe received his B.S., M.S., and Ph. D. degrees in Electronic Engineering from Tohoku University, Sendai, Japan, in 1995, 1997, and 2000, respectively. From 2000 to 2002, he was a Research Fellow of the Japan Society for the Promotion of Science, and from 2003 to 2012, he was an Assistant Professor, and from 2013 to 2023, he was an Associate Professor in the Department of Electronics, Graduate School of Engineering, Tohoku University. Since 2023, he has been a Professor in the Department of Management Science and Technology, Graduate School of Engineering, Tohoku University. He has also been a Visiting Professor in the CREOL, The College of Optics and Photonics, University of Central Florida from 2010 to 2011. He has been performing research on advanced liquid crystal displays such as wide viewing angle LCD, reflective full-color LCD, field sequential color LCD, and flexible LCD. He is a fellow of the Society for Information Display.

Hiroyasu Sato received the B.E. and M.E. degrees from Chuo University, Tokyo, Japan, in 1993 and 1995, respectively, and the D.E. degree from Tohoku University, Sendai, Japan, in 1998. He is currently an Assistant Professor with the Department of Communications Engineering, Tohoku University. His current research interests include the experimental study of electromagnetic waves, computational electromagnetics, antennas in plasma, antennas for plasma production, broadband antennas, wireless power transfer, and active/passive millimeter wave imaging. He is a member of the Institute of Electronics, Information and Communication Engineers (IEICE). He received the First Place of the Best Paper Award from the International Symposium on Antennas and Propagation (ISAP), in 2017. He is a member of the Institute of Electronics, Information and Communication Engineers (IEICE).

Qiang Chen received the B.E. degree from Xidian University, Xi'an, China, in 1986, the M.E. and D.E. degrees from Tohoku University, Sendai, Japan, in 1991 and 1994, respectively. He is currently Chair Professor of Electromagnetic Engineering Laboratory with the Department of Communications Engineering, Faculty of Engineering, Tohoku University. His primary research interests include antennas, microwave and millimeter wave, electromagnetic measurement and computational electromagnetics. He received the Best Paper Award and Zen-ichi Kiyasu Award from the Institute of Electronics, Information and Communication Engineers (IEICE). He served as the Chair of IEICE Technical Committee on Photonics-applied Electromagnetic Measurement from 2012 to 2014, the Chair of IEICE Technical Committee on Wireless Power Transfer from 2016 to 2018, the Chair of IEEE Antennas and Propagation Society Tokyo Chapter from 2017 to 2018, the Chair of IEICE Technical Committee on Antennas and Propagation from 2019 to 2021. IEICE Fellow.

Hideo Fujikake received M.E and Ph.D. degrees from Tohoku University, Japan, in 1985 and 2003, respectively. In 1985, he joined Japan Broadcasting Corporation (NHK) and he was with NHK Science and Technology Research Laboratories In 1988-2012. He was a Visiting Professor at Tokyo University of Science in 2006-2012. Since 2012, he has been a Professor at Department of Electronic Engineering, Tohoku University. His interest has been concerned with various functional liquid crystal devices. He received Best Paper Awards from Institute of Electronics, Information and Communication Engineers (IEICE) in 2001 and 2017, Best Paper Awards from Japanese Liquid Crystal Society (JLCS) in 2001 and 2015, Niwa-Takayanagi Best Paper Awards from Institute of Image Information and Television Engineers of Japan (ITE) in 2003 and 2009. He also obtained Achievement Awards from IEICE, ITE and JLCS in 2022, 2018 and 2017. He served as a General Chair in International Display Workshops (IDW) in 2021, a Japan Chapter Chair in IEEE Consumer Electronics Society in 2012-2014, and a Vice President of JLCS in 2015-2016. He is an IEICE fellow since 2015, ITE fellow since 2016, and JSAP (Japan Society of Applied Physics) fellow since 2019.